Local Dynamic Combustion Model Adaptation for Large-Eddy Simulation of Scramjets at Reduced Cost

Matthew Bonanni[a], Andrew Norris[b], and Matthias Ihme[a,c]

[a]Department of Mechanical Engineering, Stanford University
440 Escondido Mall, Stanford, California, United States of America

[b]NASA Langley Research Center
1 NASA Dr, Hampton, Virginia, United States of America

[c]Department of Photon Science, SLAC National Accelerator Laboratory
2575 Sand Hill Rd, Menlo Park, California, United States of America

1 Introduction

The application of large-eddy simulation (LES) to scramjet combustors is rendered prohibitively expensive by the difficulty of simulating supersonic combustion. Finite-rate chemistry (FRC) approaches, while offering high fidelity, are often cost-prohibitive in scramjet simulations due to the grid resolutions required for an adequately-resolved LES of the complex compressible turbulence. Additionally, increased interest in the use of storable hydrocarbon propellants exacerbates this problem by the increased complexity of their chemical mechanisms. In contrast, typical flamelet models and other low-dimensional manifold models offer reduced computational cost, but are inadequate in representing complex combustion processes, including significant pressure variations, flame/wall coupling, and transient ignition and shock/flame coupling that occurs in this context.

The Pareto-efficient combustion (PEC) framework [1] addresses this issue by dynamically assigning different combustion submodels in local regions of the computational domain. These are selected from a user-specified set of candidate combustion submodels, based on user-specified quantities of interest (QoIs) whose error is to be minimized. A user-defined parameter allows for adjusting the cost of the simulation to favor more or less expensive models. This framework enables tailoring the model assignment to specific applications, including the prediction of emissions, ignition, and spray combustion [2, 3, 4]. This framework has been successfully applied to low-Mach simulations such as turbulent jet flames, where it has been demonstrated to significantly improve CO prediction compared to flamelet models at less than half the cost of a full FRC simulation, by applying FRC to only 9% of the domain [2]. As an expansion on earlier work applying the PEC framework to a scramjet engine [5], the present work presents comparisons with a full finite-rate chemistry simulation for the purpose of validation.

Correspondence to: mbonanni@stanford.edu

2 Computational Approach

The LES presented in this work numerically solves the fully-compressible, Favre-filtered conservation equations of mass, momentum, energy, and chemical species:

$$\partial_t \overline{\rho} + \nabla \cdot (\overline{\rho}\widetilde{\mathbf{u}}) = 0, \tag{1}$$

$$\partial_t (\overline{\rho}\widetilde{\mathbf{u}}) + \nabla \cdot (\overline{\rho}\widetilde{\mathbf{u}}\widetilde{\mathbf{u}} + \overline{p}\mathbf{I}) = \nabla \cdot \left(\overline{\tau} + \tau_{\text{sgs}}\right), \tag{2}$$

$$\partial_t \left(\overline{\rho}\widetilde{E}\right) + \nabla \cdot \left(\overline{\rho}\widetilde{E}\widetilde{\mathbf{u}} + \overline{p}\right) = \nabla \cdot \left[\left(\overline{\tau} + \tau_{\text{sgs}}\right) \cdot \widetilde{\mathbf{u}} - \left(\overline{\mathbf{q}} + \mathbf{q}_{\text{sgs}}\right)\right], \tag{3}$$

$$\partial_t \left(\overline{\rho}\widetilde{\boldsymbol{\phi}}^m\right) + \nabla \cdot \left(\overline{\rho}\widetilde{\mathbf{u}}\widetilde{\boldsymbol{\phi}}^m\right) = -\nabla \cdot \left(\overline{\mathbf{j}} + \mathbf{j}_{\text{sgs}}\right) + \overline{\mathbf{S}}_\phi, \tag{4}$$

where ρ is the density $\mathbf{u}$ is the velocity vector, p is the pressure, τ is the stress tensor, E is the total energy, and $\mathbf{q}$ is the heat flux; $\boldsymbol{\phi}^m$ represents the manifold-describing variables for the locally-applied combustion submodel m, with corresponding flux vector $\mathbf{j}$ and chemical source term $\mathbf{S}_\phi$.

A detailed description of the PEC framework is presented in [1]. PEC determines the submodel assignment for each cell in the computational domain using a global algorithm, which minimizes the total error of the simulation subject to a total cost constraint [4].

The error represents the local difference between the true state $\boldsymbol{\phi}^m$ and the modeled state $\hat{\boldsymbol{\phi}}^m$ for a particular submodel m. In order to avoid the need for knowledge of the true state, which would require a high-fidelity reference simulation, thereby negating the benefits of the dynamic submodel assignment, a so-called drift term of QoI ψ and model m, $\widetilde{\mathcal{D}}_\psi^m$, is computed for a particular process of interest (PoI) $\widetilde{\pi}$, which has sensitivities to a set of QoIs, $Q = \left\{\widetilde{\psi}_1, \ldots, \widetilde{\psi}_{N_Q}\right\}$:

$$\widetilde{\mathcal{D}}_\psi^m = \overline{\rho}\widetilde{D}_t\widetilde{\psi}|_{\widetilde{\psi}=\widetilde{\psi}^m} - \overline{\rho}\frac{\partial\widetilde{\psi}^m}{\partial\widetilde{\boldsymbol{\phi}}^m} \cdot \widetilde{D}_t\widetilde{\boldsymbol{\phi}}^m, \tag{5}$$

$$\widetilde{\mathcal{D}}_\pi^m = \sum_{i=1}^{N_\pi} \widetilde{\frac{\partial\pi}{\partial\psi_{\pi,i}}\mathcal{D}_{\psi_{\pi,i}}^m}, \tag{6}$$

where $\widetilde{\psi}^m$ is the QoI evaluated using the solution of model m. This drift term describes the growth rate of the manifold error, where the first term represents the material derivative of the QoI as predicted by a high-fidelity reference submodel, and the second term is the material derivative of the QoI as predicted by the manifold variables of model m, $\widetilde{\boldsymbol{\phi}}^m$. The drift term for the PoI is then computed as the sum of the drift terms for each QoI, weighted by the sensitivities of the PoI to each QoI.

These equations are solved using an unstructured finite volume solver [6, 7]. This solver uses a nominally fourth-order scheme for the viscous fluxes, and a sensor-based hybrid scheme for the Euler fluxes. A simple balancing splitting scheme is used for time-stepping, with a third-order strong stability preserving Runge-Kutta scheme being used for the non-stiff terms while a fourth-order semi-implicit Rosenbrock-Krylov scheme is used for the stiff reaction terms of the FRC submodel [8]. Numerical instabilities at discontinuities are avoided via a shock sensor based on density gradients, with a 2nd order essentially-non-oscillatory scheme being used in these regions. Isothermal, ODE-based wall models are used at each of the walls of the domain.

The set of candidate submodels for the PEC framework in this study comprises an FRC model using the 23-species skeletal ethylene-air mechanism of Zettervall et al. [9] and a flamelet-progress variable (FPV) model computed from this mechanism [10].

3 Experimental Configuration

The present work simulates the ethylene-fueled, cavity-stabilized model scramjet combustor at Research Cell 19 at Wright-Patterson Air Force Base [11]. This configuration is depicted in Fig. 1. The present work considers the configuration of eleven spanwise injectors in the cavity ramp region, which has been most commonly applied in this facility [12, 13].

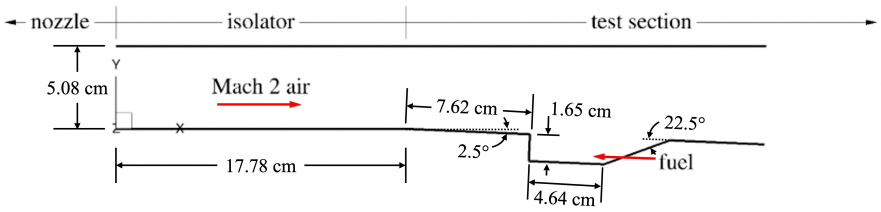

Figure 1: Schematic of the model scramjet combustor at the RC19 facility, WPAFB, adapted from [14].

The inlet air is supplied at Mach 2.0 by the RC19 facility nozzle [11]. The stagnation pressure and temperature of the incoming airflow are 483 kPa and 589 K, respectively. Ethylene fuel is injected through the injectors at 56 SLPM.

4 Computational Configuration

4.1 Domain

To reduce the computational cost, a spanwise periodic section containing two of the eleven injectors was isolated for this simulation, as in the work of Peterson et al. [14]. The domain captures a section of the flowpath beginning with the point where the bottom wall of the combustor begins to ramp downwards, and ending approximately 5 cm past the lip of the cavity ramp. Each injector was extended to a length $L = 1.5$ cm for $L/D \geq 5$, instead of modeling the full fuel plenum. A structured mesh with 5.1 million cells was developed for this domain, having a minimum grid spacing of 50 $\mu\mathrm{m}$ at the walls. This corresponds to a y^+ value of 50, which is suitable for the WMLES approach applied here.

4.2 Boundary Conditions

A subsonic mass flux-enforcing boundary condition is used for the fuel injectors, while the air inflow is injected with turbulence and a boundary layer profile derived from hybrid RANS-LES simulations performed by Peterson et al. [14]. All walls in this simulation are isothermal at a temperature of 300 K, and a supersonic boundary condition is applied at the outlet.

In this preliminary simulation, for the PEC combustion framework, four QoIs are considered: the mass fractions of CO, CO_2, H_2, and H_2O, each with equal weight. These have been selected because they correspond to the constitutive species of the progress variable, and are involved in the most significant exothermic reactions, thereby serving as a proxy for heat release [15].

5 Results

Contour plots of instantaneous and time-averaged results for this simulation are presented in Fig. 2. Here, we note the high-temperature turbulent combustion occupying the cavity. In the shear layer, turbulent mixing entrains air into the cavity and combustion occurs in this well-mixed region. The combustion submodel assignment is also depicted as an instantaneous snapshot in coordination with a time-averaged probability of FRC assignment. Finite-rate chemistry is applied to less than 11% of the domain, while FPV is applied everywhere else. There are two primary locations where FRC is applied: the turbulent shear layer and a portion of the cavity surrounding the point of injection. This aligns with expectations that these regions are chemically and hydrodynamically complex, so the FPV model underperforms. The strong flame interaction effects and significant pressure variations are both unaccounted for in standard flamelet models like the one used here, so FRC is required to accurately model these regions.

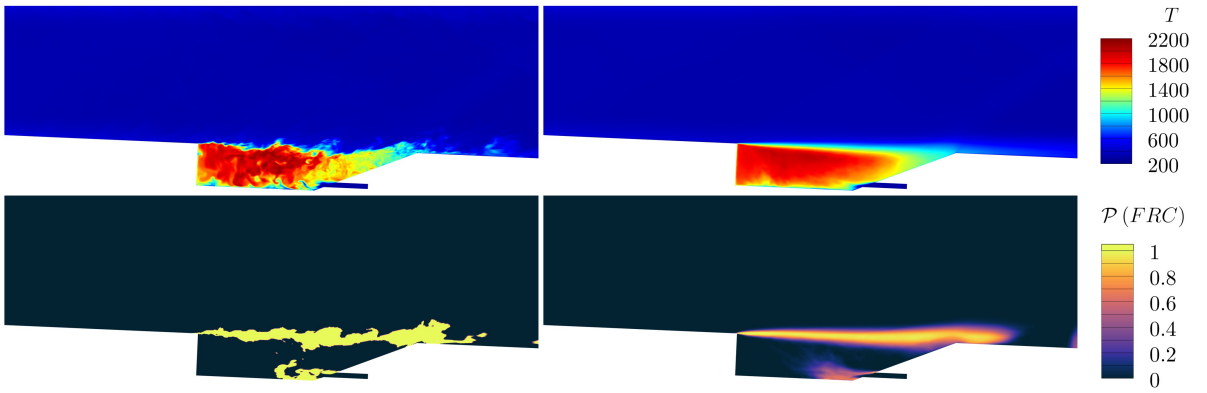

Figure 2: Instantaneous (left) and time-averaged (right) contours of temperature (top, K) and submodel assignment (bottom) in the mid-plane section of the large-eddy simulation.

A comparison of the results from the PEC simulation and a full FRC simulation are presented in Fig. 3. Here, we note good agreement in time-averaged contours of axial velocity, temperature, and heat release is achieved via PEC's application of FRC to less than 11% of the computational domain. We additionally note that in both cases, the heat release rate is largely localized in the shear layer, especially near the upstream lip of the cavity, as well as a small region near the fuel injector. By comparison with Fig. 2, we note a correlation between the heat release and the application of FRC. This indicates that the PEC framework is correctly identifying the most chemically-active regions of the domain through the selection of products of major exothermic reactions as QoIs.

6 Conclusions

This study builds on prior work using the PEC framework for supersonic combustion. We have demonstrated that, via the selection of progress variable species as QoIs, we have successfully isolated the most chemically-active regions of the domain and locally applied FRC modeling in these regions. Furthermore, these regions represent locations where the complexities of supersonic combustion are especially present, which the low-order tabulated chemistry approach is unable to effectively model. We have additionally demonstrated that the results of this simulation, while applying FRC to less than 11% of the computational domain, agree with the results of a full finite-rate chemistry simulation in the regions of most significant heat release.

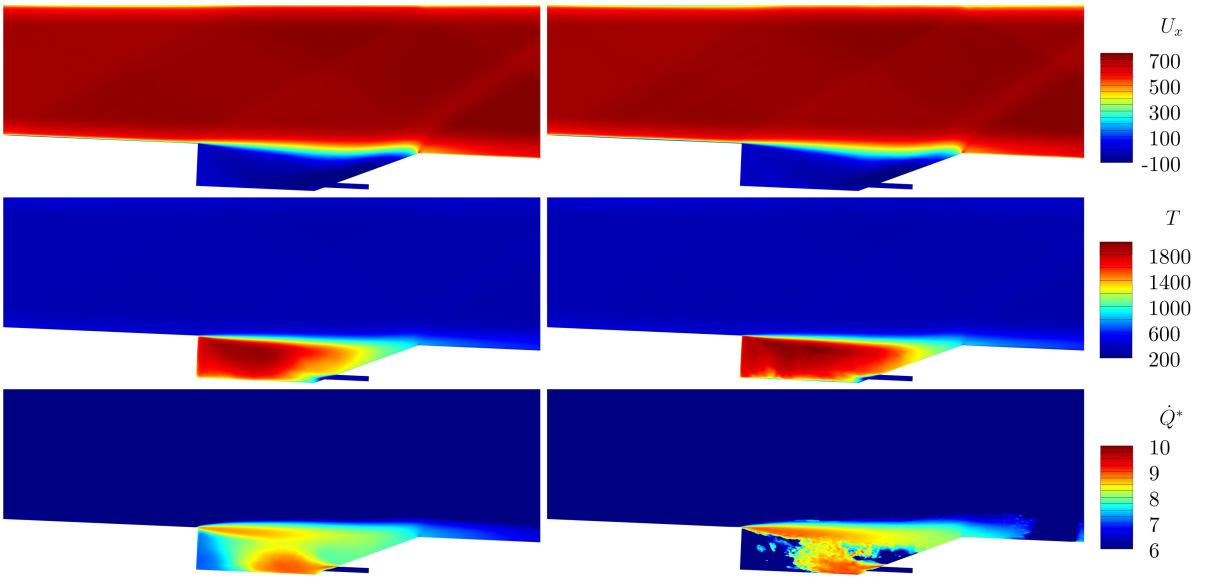

(a) FRC (b) PEC (11% FRC)

Figure 3: Comparison of time averaged contours of temperature (top, K), axial velocity (center, $\mathrm{m\,s^{-1}}$), and signed magnitude heat release rate $\dot{Q}^* = \mathrm{sign}(\dot{Q})\log_{10}(1 + |\dot{Q}|)$ (bottom) for a full finite-rate chemistry simulation (a) and the PEC simulation (b). On average, the PEC simulation applies finite-rate chemistry to less than 11% of the domain.

Acknowledgements

Financial support by the NASA Fellowship Activity program, training grant #80NSSC21K2054, is gratefully acknowledged. The authors also thank Drs. David Peterson, Timothy Ombrello, and Campbell Carter of the Air Force Research Laboratory for sharing the turbulent inflow data and for technical discussions.

References

[1] H. Wu, Y. C. See, Q. Wang, and M. Ihme, "A Pareto-efficient combustion framework with submodel assignment for predicting complex flame configurations," *Combust. Flame*, vol. 162, no. 11, pp. 4208–4230, nov 2015.

[2] H. Wu, P. C. Ma, T. Jaravel, and M. Ihme, "Pareto-efficient combustion modeling for improved CO-emission prediction in LES of a piloted turbulent dimethyl ether jet flame," *Proc. Combust. Inst.*, vol. 37, no. 2, pp. 2267–2276, jan 2019.

[3] Q. Douasbin, M. Ihme, and C. Arndt, "Pareto-efficient combustion framework for predicting transient ignition dynamics in turbulent flames: Application to a pulsed jet-in-hot-coflow flame," *Combustion and Flame*, vol. 223, pp. 153–165, 2021.

[4] D. Mohaddes, D. Brouzet, and M. Ihme, "Cost-constrained adaptive simulations of transient spray combustion in a gas turbine combustor," *Combustion and Flame*, 2023, in press.

[5] M. Bonanni, A. Norris, and M. Ihme, "Adaptive Modeling of Supersonic Combustion in a Cavity-Stabilized Scramjet," in *AIAA SciTech Forum*, National Harbor, MD, Jan. 2023.

[6] Y. Khalighi, J. W. Nichols, S. K. Lele, F. Ham, and P. Moin, "Unstructured large eddy simulation for prediction of noise issued from turbulent jets in various configurations," in *17th AIAA/CEAS Aeroacoustics Conf. 2011 (32nd AIAA Aeroacoustics Conf.*, 2011.

[7] P. C. Ma, Y. Lv, and M. Ihme, "An entropy-stable hybrid scheme for simulations of transcritical real-fluid flows," *J. Comput. Phys.*, vol. 340, pp. 330–357, jul 2017.

[8] H. Wu, P. C. Ma, and M. Ihme, "Efficient time-stepping techniques for simulating turbulent reactive flows with stiff chemistry," *Comput. Phys. Commun.*, vol. 243, pp. 81–96, oct 2019.

[9] N. Zettervall, C. Fureby, and E. J. K. Nilsson, "Small Skeletal Kinetic Reaction Mechanism for Ethylene–Air Combustion," *Energy & Fuels*, vol. 31, no. 12, pp. 14 138–14 149, Dec. 2017, publisher: American Chemical Society.

[10] M. Ihme, C. M. Cha, and H. Pitsch, "Prediction of local extinction and re-ignition effects in non-premixed turbulent combustion using a flamelet/progress variable approach," *Proc. Combust. Inst.*, vol. 30, pp. 793–800, 2005.

[11] M. R. Gruber and A. S. Nejad, "New supersonic combustion research facility," *J. Propuls. Power*, vol. 11, no. 5, pp. 1080–1083, 1995.

[12] T. Ombrello, E. Hassan, C. Carter, B. McGann, T. Lee, H. Do, D. Peterson, P. Ivancic, and E. Luke, "Establishing the controlling parameters of ignition in high-speed flow," in *AIAA SciTech Forum*, no. January, San Diego, CA, 2016, AIAA-Paper 2016-0658.

[13] S. Okhovat, T. Ombrello, and M. I. Resor, "Radiance of select species in a scramjet cavity," in *AIAA SciTech Forum*, Grapevine, TX, 2017, AIAA-Paper 2017-0340.

[14] D. M. Peterson, E. Hassan, S. G. Tuttle, M. Hagenmaier, and C. D. Carter, "Numerical investigation of a supersonic cavity flameholder," in *AIAA SciTech Forum*, no. January, National Harbor, MD, 2014, AIAA-Paper 2014-1158.

[15] M. Ihme, L. Shunn, and J. Zhang, "Regularization of reaction progress variable for application to flamelet-based combustion models," *J. Comput. Phys.*, vol. 231, pp. 7715–7721, 2012.